DYNAMIC ELECTROMECHANICAL RESPONSE OF 4H AND 6H SINGLE CRYSTAL SILICON CARBIDE

Leslie Lamberson
Department of Mechanical Engineering & Mechanics, Drexel University
Philadelphia, PA, USA

ABSTRACT

Ceramic materials are used extensively in armor applications for both solider and vehicle protection. Certain ceramics, such as silicon carbide, exhibit piezoelectricity, however the coupling between mechanical and electrical fields is not currently utilized. This paper highlights a unique experimental methodology that measures the in-situ electromechanical response of single crystal 4H and 6H silicon carbide (SiC) under dynamic compression using a Kolsky (Split-Hopkinson) bar at strain rates of $10^3$ $s^{-1}$. Mapping of both the damage evolution and electric charge during rapid loading and fragmentation of these two polytypes is presented and discussed in the context of the wurtzite crystal structure.

INTRODUCTION

Silicon carbide crystallizes in either a cubic or hexagonal form with over 250 polymorphs.[1, 2] In the case of the 4H and 6H hexagonal polytypes, strong covalent bonding between the silicon and the carbide give SiC its high strength properties along with high resistance to temperatures and radiation; while its noncentrosymmetric structure gives rise to its piezoelectric properties.[3, 4] The 4H and 6H polytypes consist of stacking sequence layers that differ, resulting in three inequivalent sites with a small variation in band gap and lattice parameters, leading to variations in the resulting electromechanical properties.[5] In a characteristic sequence both 4H and 6H exhibit a single hexagonal bond, but 6H has two quasi-cubic bonds and 4H only one.[6] The bending, or breaking of the hexagonal bond in the case of failure resulting from impact, is what produces to the intrinsic electrical response (from the direct piezoelectric effect). The bond architecture alone suggests that the mechanical response under compression may be greater in the 6H polytype, but the electric response would remain the same for both 6H and 4H. As a result, the goal of this paper is to examine dynamic compressive deformation and damage of 4H and 6H SiC, and determine its coupled electrical response.

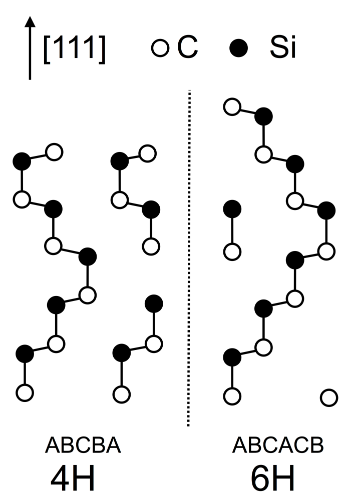


Figure 1. Stacking sequence of the 4H and 6H polytypes of SiC. The atomic structures are described in the $(10\bar{1}0)$ hexagonal plane where A, B, and C denote a bilayer. Figure adapted from Park, et al.[4]

## BACKGROUND

While a substantial amount of research has been conducted on the synthesis of monocrystalline silicon carbide, with particular effort on 6H due to its relevance in the semiconductor and electronics industry, epitaxial development and characteristics will not be emphasized here.[7, 8] Rather, the failure of silicon carbide under various loading conditions in regards to the microstructure will be the focus. For monocrystalline silicon carbide, Karch and colleagues used ab initio density-functional-perturbational-theory to show that while the structural and electronic properties are very similar for the hexagonal polytypes of silicon carbide and the ground-state properties are rather independent of polytype, increasing the hydrostatic pressure exhibits a pressure-dependence on the resulting dynamical and dielectric properties.[9] Clayton developed an electromechanical model to describe the behavior of single crystal 6H SiC and used it to predict the response of crystals under planar shock loading conditions; determining that the mechanical stress response is negligibly influenced by the piezoelectric effect in small strains, but the influence of nonlinear elastic third order constants and anisotropy are potentially significant.[10]

An extensive amount of work has been conducted experimentally on the dynamic mechanical response of various forms of bulk silicon carbide, typically hot pressed versions with a variety of sintering agents. Under high strain-rate conditions, the overall compressive response of a brittle ceramic has been shown to be dependent on inertial effects related to the propagation of cracks.[11-14] Yet at the same time, plasticity mechanisms have been shown for brittle ceramics under various confinement and extreme loading conditions.[15-18] Bourne and colleagues conducted plate impact and Kolsky bar (split-Hopkinson pressure bar SHPB) test on three grades of bulk silicon carbide and presented data which indicated that material failure was delayed after the maximum stress had been achieved in the samples.[19] Shih and colleagues examined two types of hot pressed silicon carbide, one with carbon and boron sintering agents, and the other aluminum, under dynamic compressive conditions using a Kolsky (SHPB) and under confinement with high-velocity impacts by a cylindrical tungsten alloy rod. This study demonstrated plastic deformations of dislocations and stacking faults, and the flaws and defect evolution under loading as a consequence of the sintering agents.[20] Sarva and Nemat-Nasser conducted tests on a Kolsky bar and a quasi-static universal testing machine to show an increase in the compressive strength of hot-pressed sintered SiC above $10^2$ $s^{-1}$, although the failure modes appeared similar in both loading regimes.[21] Wang and Ramesh used a modified Kolsky bar technique along with standard quasi-static compressive testing confirming the inertia effect is responsible for the rate response in hot-pressed silicon carbide, SiC–N, while subcritical crack growth is the dominant effect of loading in the quasi-static regime.[22] Damaged but interlocked hot-pressed silicon carbide was examined using a modified Kolsky bar by Luo and colleagues, where a double stress pulse was loaded into the specimen. While the damaged ceramic was insensitive to increasing strain rates, further damage was shown with increasing lateral confinement.[23]

At a higher strain-rate regimes, several sintered variants of silicon carbide were examined for cavity expansion behavior under impact from tungsten carbide spheres at 1700 m/s by Normandia.[24] Granulated silicon carbide examined by Klopp and Shockey under pressure-shear plate impact at shear strain rates of $10^5$ $s^{-1}$ and mean stresses ranging from 1-9 GPa demonstrated a coefficient of friction that was 50% less than the quasi-static value.[25] Further shock experiments by Grady were conducted to determine the Hugoniot precursor characteristics and the wave dynamics of polycrystalline silicon carbide, and a Hugoniot elastic limit of 15 GPa was reported.[26] Gupta and colleagues have conducted a number shock studies on polycrystalline SiC, demonstrating peak stresses of 7.3 to 23 GPa and a Hugoniot elastic limit of 11.7 GPa.[27-29] The Hugoniot and strength behavior of two varieties of silicon carbide were also examined by Volger and colleagues demonstrating the material strength increases by 50% at stresses of 50-75 GPa before decreasing as the phase transformation is approached.[30] Hypervelocity impact experiments by Behner and colleagues impacting SiC-N ceramics with long gold rods at 2.0 to 6.2 km/s suggested an increase in penetration resistance of the material at impact velocities greater than roughly 4.5 km/s.[31] The aforementioned studies demonstrate the dramatic effects the microstructure and loading conditions have on the global response of the material under high strain-rates. The effect of electromechanical forces on the response of single crystal silicon carbide has, to the author's knowledge, not been explored experimentally under dynamic loading conditions prior to this study.

## MATERIAL AND TEST METHODOLOGY

A Kolsky compression bar (SHPB) 25 mm in diameter was used to characterize the electromechanical response of the single crystal silicon carbide at high rates, as shown in Figure 2. A striker bar is ejected from a pressurized gas gun and impacts an incident bar, sending an elastic compressive pulse down the bar. Once at the sample, part of the pulse is reflected, and the remaining part is transmitted through the sample into the transmission bar. Strain gauges on the incident and transmission bars capture the incident, reflected, and transmitted wave signals ($\epsilon_I$, $\epsilon_R$, $\epsilon_T$), respectively. Once an equilibrium state is achieved, assuming a 1D stress state in the bar, and knowing the bar elastic modulus $E_b$ area $A_b$, and dilatational wave speed $c_b$, and the specimen length $l_0$, and impact area $A_0$ the specimen, nominal stress and strain during loading can be calculated as follows (details in referenced literature):[32]

$$\dot{\epsilon}(t) = -\frac{2c_b}{l_0}\epsilon_R(t) \Rightarrow \epsilon(t) = \int_0^t \dot{\epsilon}(\tau)d\tau \tag{1}$$

$$\sigma(t) = \frac{E_b A_b}{A_0}\epsilon_T(t)\ . \tag{2}$$

To accurately investigate the deformation of the single crystals, the following modifications were applied to the Kolsky setup: a copper pulse shaper was placed in front of the incident bar to ensure a uniform stress, and a pair of contact platens is used to prevent damage in the incident and transmission bars on each side of the sample.[33, 34] The platens were chosen to match the geometry impedance of the bars ($\rho c_b A_0$, where $\rho$ is the density of the bar). Tests used either alumina ($Al_2O_3$) platens or tungsten carbide (WC) platens, and the striker, incident and transmission bars are made of heat-treated maraging steel.

Fairfield Crystal Technology of New Milford, Connecticut provided single crystal discs with a polish on the c-axis face of 3 microns or less, made from 6H and 4H (0001) boules. The discs were sent to Bomas Machine Specialists in Summerville, Massachusetts and machined into cuboidal Kolsky (SHPB) samples. Due to the limitations of crystal growth techniques the samples were of limited size, and were cut from the thickest portion of the discs as 3.5x3.5x4 mm samples for 6H, and 2x2x2.5 mm samples for 4H. All samples were impacted along the c-axis (primary piezoelectric axis) to induce the largest electrical response. Noticeable flaws were present in the crystals, particularly towards the edges of the disc, which appeared as opaque particles, so care was taken to cut samples from the most transparent and homogeneous sections (see Figure 3). The basic elastic, crystallographic and electric properties of the crystals are listed in Table I.

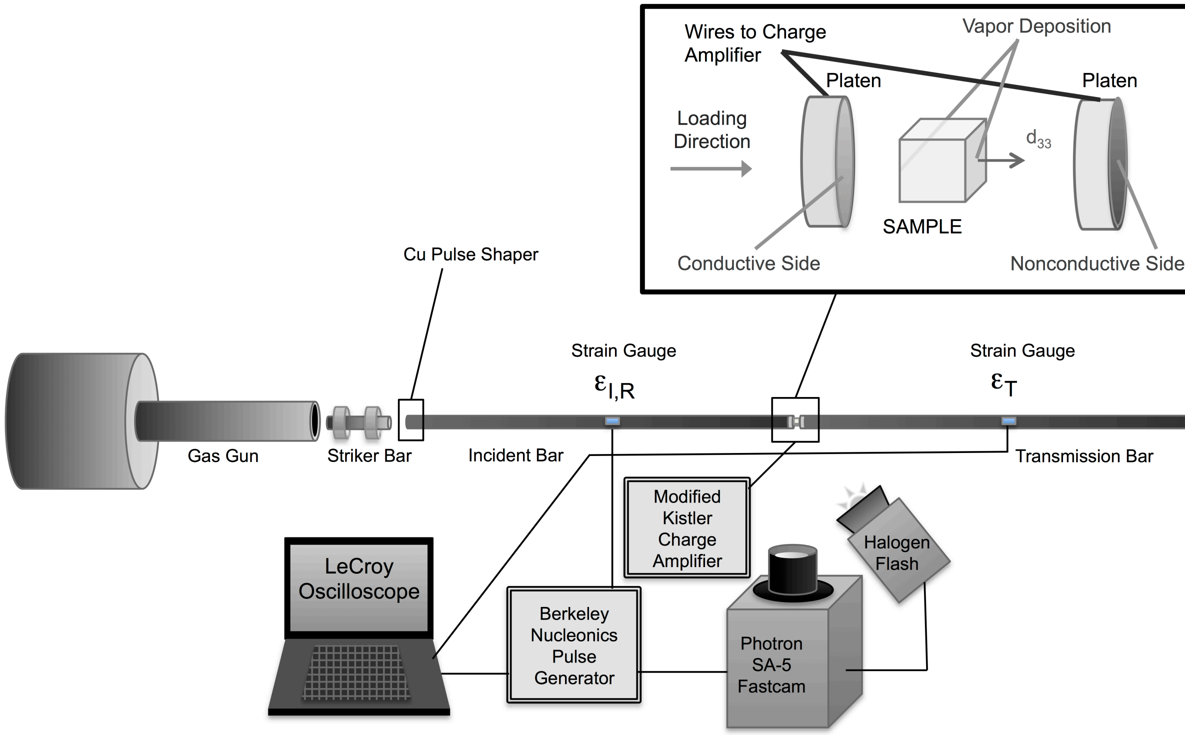


Figure 2. Schematic highlighting the experimental setup used to study the dynamic electromechanical response of single crystal silicon carbide.

Prior to testing, the uprange and downrange faces of the silicon carbide samples had electrodes vapor deposited in a cleanroom chamber under high vacuum. These electrodes consisted of a 10 nm layer of chromium, followed by 200 nm layer of aluminum (copper deposition was avoided due to oxidation concerns). Electrical shielding of the sample was necessary as the Kolsky bars are conductive. To ensure isolation of the electrical signal, the platens were modified, and the experimental system ground with the electrical measurement isolated to only the sample region of interest. Early tests used platens of alumina ($Al_2O_3$) polished to 3 microns, and then vapor deposited on the sides that mated with the crystal sample. Thin-gauge wire (20AWG) was attached to the platen using silver paste that connected a low-noise shielded cable attached to a Kistler charge amplifier (with the bandpass filter bypassed). The electrical response was recorded on the charge amplifier in a short time-scale charge mode. High-speed imaging with a Photron SA-5 Fastcam was used to capture the evolving damage, as well as ensure that the platens maintained structural integrity during the loading. Both cases of catastrophic failure from the impact loading, and only partial fragmentation from less-than-catastrophic failure were explored. In cases of catastrophic failure, the sample failed by being unable to withstand additional compressive loading and consequently comminuting, and not due to premature platen failure. Preliminary tests with the added electrical measurement components were conducted on alumina (a non-piezoelectric ceramic) to confirm no false or wandering electrical signals, and ensure measurements taken on the crystals were from the piezoelectric effect. Other preliminary tests were conducted to ensure that no charge was registered due to potential fractoluminescence.

Table I. Basic crystal, elastic and electrical properties of single crystal (4H) and (6H) SiC. [35-38]

| | Density ($g/cm^3$) | Dilatational wave speed [001] (km/s) | Lattice Constants (Å) | | Piezoelectric coefficient | | Bandgap (eV) |
|---|---|---|---|---|---|---|---|
| | | | a | c | $e_{33}$ ($C/m^2$) | $d_{33}$ (pC/N) | |
| 4H SiC | 3.21 | 13.1 | 3.07 | 10.08 | 0.33* | 9.7 | 3.2 |
| 6H SiC | 3.21 | 13.1 | 3.073 | 15.12 | 0.2 | 9.7 | 3.0 |

*Theoretically predicted.

Later tests were conducted with tungsten carbide (WC) platens 1.25 mm thick in order to verify the response was not affected by the presence of the platens. The WC platens were placed between the sample, and a thin (90 microns, thick enough to avoid punch-through effects) Mylar sheet was placed between the platen and the incident or transmission bar to avoid conduction. In every test, conductive grease was used between the sample and the platens, and nonconductive grease between the bars and the platens to reduce frictional effects. It is important to note that due to the additional experimental modifications used to obtain the electrical in-situ response under dynamic loading conditions, these tests should not be taken as a direct measurement of the dynamic compressive strength of the single crystal polytypes. The results presented are, most likely, an underestimate of the overall dynamic compressive material strength due to the additional layers between the bars and the sample for electrical shielding and measurement, as well as the vapor deposition layer on the uprange and downrange ends of the sample which could cause potential residual stress concentrations. Raw voltage signals of the incident, reflected and transmitted pulses were examined post-mortem to make sure the test maintained a dynamic uniform stress state during loading, and that the 1D stress state assumption was upheld. Figure 3 illustrates the disc material as received from the vendor, as well as the cut cuboidal test sample and orientation of loading.

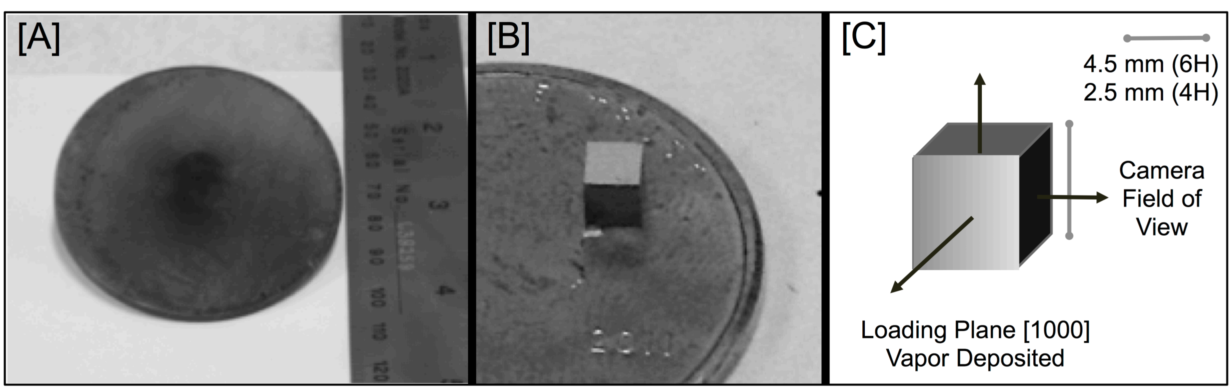


Figure 3. [A] Photo of the 4H SiC disc (approximately 66 mm in diameter, averaging 4.5 mm in thickness) [B] Photo of the cuboidal cut 4H sample with vapor deposition shown on a penny for scale [C] Schematic of the sample as oriented for experimental testing and damage visualization.

The coupling between the mechanical and electrical response in noncentrosymmetric piezoelectric crystals is mathematically described by piezoelectric theory. The electroelastic coupled relationship is defined as:[3]

$$\sigma_{ij} = C_{ijmn}\epsilon_{mn} - e_{nij}\phi_{,n} \tag{3}$$
$$D_i = e_{imn}\epsilon_{mn} + \kappa_{in}\phi_{,n} \tag{4}$$

where the stress, strain, charge density, are noted as $\sigma$, $\epsilon$, D, and $C$ and $\kappa$, are the elastic and dielectric moduli, respectively. The electric field, E, is assumed to be derived from the electric potential, $\phi$, and the piezoelectric coefficient $e$ can be related to the piezoelectric coefficient $d$ via the compliance tensor S by:

$$d_{ijm} = S_{ijkl}e_{klm}. \tag{5}$$

To simplify the notation, the elastic and piezoelectric coefficient tensors are written in reduced form employing Voight notation, so the direct relationship used in the analysis, assuming no initial electric field and that the area remains constant during testing, is expressed as a function of charge and force, F, as:[39]

$$d_{ij} = \left(\frac{\partial D_i}{\partial F_j}\right). \tag{5}$$

RESULTS AND DISCUSSION

Dynamic compression tests were conducted using a modified Kolsky bar setup (SPHB) to explore damage and the coupled electromechanical field response for 4H and 6H silicon carbide single crystals. In the case of both 4H and 6H, results indicate that a potential threshold exists in which the sample transitions to complete resistivity breakdown as a function of damage. Breakdown was not seen in impact cases on 4H when the initial pulse comminuted the specimen and on 6H when the initial pulse did not comminute the specimen. This may be explained by the fact that the physical pathways available for electron transport are being rapidly destroyed, so the sample response becomes like a transport theory problem. The breakdown could be attributed to the dynamic increasing number of nonlinearities from the growing crack fronts that coalesce, allowing electrons from broken bonds to be released, taking advantage of the semiconductor bandgap. When considering the dynamics of failure of brittle ceramics under rapid compressive loading conditions, within less than 20 microseconds, the sample appears to have little damage near post-peak stress, to a full field of dominant axial cracks running the length of the sample near the peak stress, to rapid fragmentation and failure where inertia and resulting damage essentially destroys the electrodes. Testing to failure did not result in open circuit behavior during unloading; rather it exhibited more of a short circuit behavior, which suggests the electrical connection, or lack thereof, from the damage of the mechanical loading process is not the cause of the breakdown response.

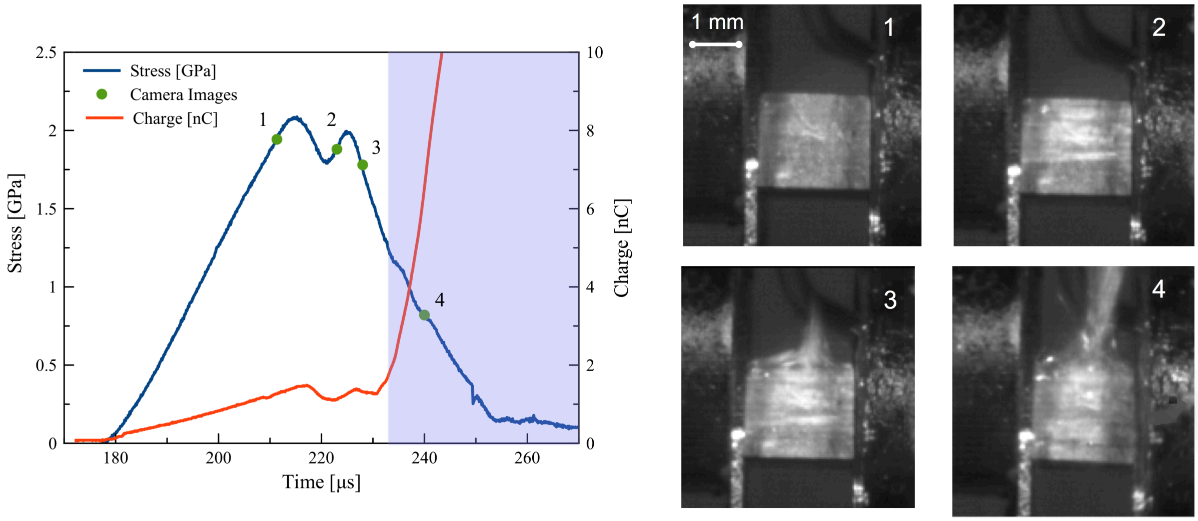


Figure 4. Dynamic electromechanical compression test result on 4H SiC where an apparent threshold (in shadow) was reached shortly after the post-peak mechanical load and electric breakdown is seen on a sample compressed below the overall failure strength, but beyond the onset of damage. For the loading portion of the impulse, the piezoelectric coefficient measured 0.12 pC/N.

Another potential source adding to the breakdown seen during the unloading portion of the curve could be the dielectric breakdown of air as damage increases. Figure 4 highlights the dynamic elastic and inelastic response during compressive test on 4H SiC below the overall catastrophic failure strength, but above onset of damage, where the post-peak electric behavior appears to increase without bounds. In the cases where the damage threshold was reached and the electric response increases dramatically on unloading, the piezoelectric coefficient on the loading portion of the curve was approximately 50% less than tests where catastrophic damage was reached. Figure 5 highlights the response of 4H SiC below the threshold, and the electrical response remained in time synchronization with the mechanical load. Clearly local nonlinearities can be seen within the force-charge response in all cases, and could be due to influences of the higher order nonlinear elastic terms coming into play as suggested by Clayton,[10] but appeared more prominent on cases where breakdown was not seen. The piezoelectric coefficients were approximated by a linear curve fit, all with $R^2$ values greater than 0.95. The tests where breakdown occurred averaged an in-situ piezoelectric coefficient on loading of approximately 0.14 pC/N (+/- 0.026). In the case where the apparent threshold was not reached, the measured piezoelectric coefficient was larger, and remained essentially unchanged during loading and unloading at approximately 0.30 pC/N. This is an order of magnitude lower response than those reported in literature on pure sample grades used in the semiconductor industry by evaluating the second-order non-linear optical coefficients using the wedge technique.[38]

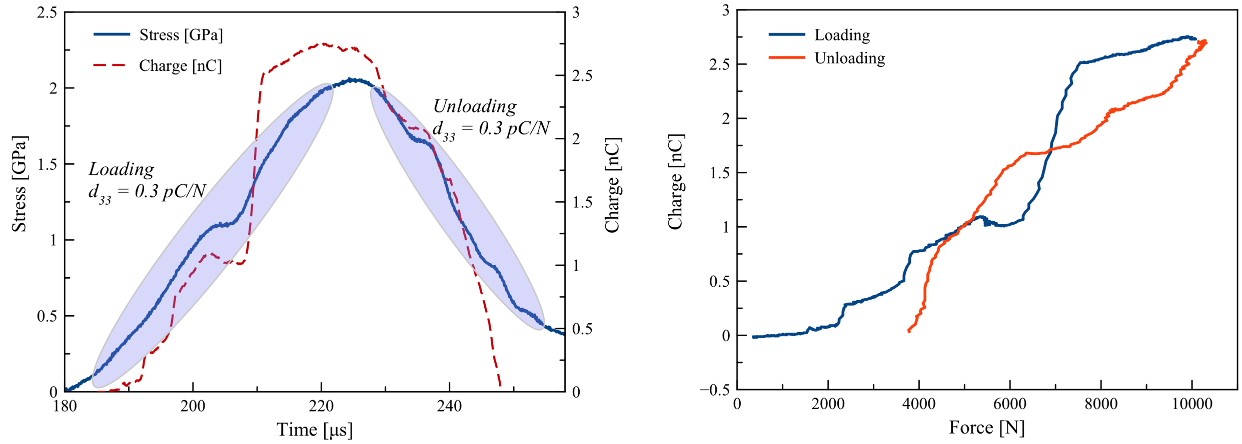


Figure 5. Dynamic electromechanical compression test of 4H SiC with no apparent threshold behavior.

The 4H and 6H crystals had a wide range of compressive strength values during testing, all of which appeared less than would be expected for the pure monocrystalline materials. As mentioned previously, this could partially be due to the modified experimental configuration that includes an electrode film vapor deposited onto the uprange and downrange faces of the sample, as well as additional layers within the platen-sample interface. It could also be due to the inherent flaws in the material. Unlike a polycrystalline material that has a stochastic distribution of flaws within the microstructure, the single crystal flaws, while potentially less in number overall, may have greater individual impact on the response. Additionally, with no (or essentially no) grain boundaries, once initiated under dynamic conditions, a flaw may more rapidly propagate and decrease the global constitutive response as it lacks potential sites within the microstructure to be pinned or otherwise hindered.

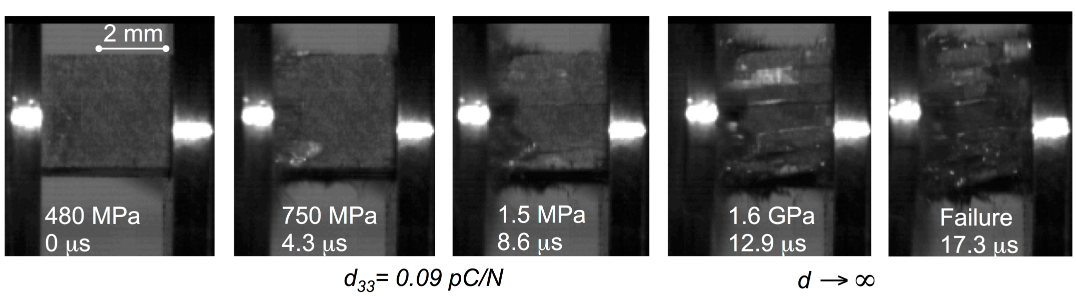


Figure 6. Dynamic electromechanical compression test result of 6H SiC where the sample failed catastrophically on the initial impact load of roughly 2 GPa, and the charge increased without bounds.

The 6H crystals appeared to the show the opposite trend from the 4H crystals, where breakdown occurred on tests where damage was initiated, but the sample did not completely comminute from the initial impact. No discernable difference in the peak compressive strength was seen in crystals that failed catastrophically on the initial impact, versus those that incurred damage but did not fail catastrophically, nor between the two polytypes examined. Both crystals exhibited the same order of magnitude of peak electrical response, however the 6H was approximately 16% higher, although not outside statistical error

The rather stochastic nature of the electromechanical behavior could be attributed to the inherent impurities in the crystals. Based on dislocation theory, the extra energy that an imperfect crystal possesses in comparison to a perfect crystal is the strain energy of the dislocations. Silicon carbide crystals are most often grown in epitaxial layers by chemical vapor deposition.[40-44] As a result, understanding the defect generation and development during the growth process is an important factor that may play an inherent role in the resulting bulk electromechanical response.[40, 42-45] Namely, defects discovered and studied in epilayer of hexagonal polytype of SiC include micropipes, threading edge dislocations, threading screw dislocations, basal plane dislocations, and low angle grain boundaries consisting of a mixture of defects and stacking faults; all of which may lead to altered behavior in bulk SiC crystals and have been shown to affect the electromechanical properties of interest here on a smaller characteristic length scale and under quasi-static conditions.[45-47] While it has been reported in literature that 6H SiC can exhibit spontaneous polarity, no polarity changes were observed these tests.[48] Figure 7 illustrates a case where the sample exhibited a very high mechanical response, but a very low electrical response, and no threshold behavior was seen. A summary of the test results can be found in Table II below.

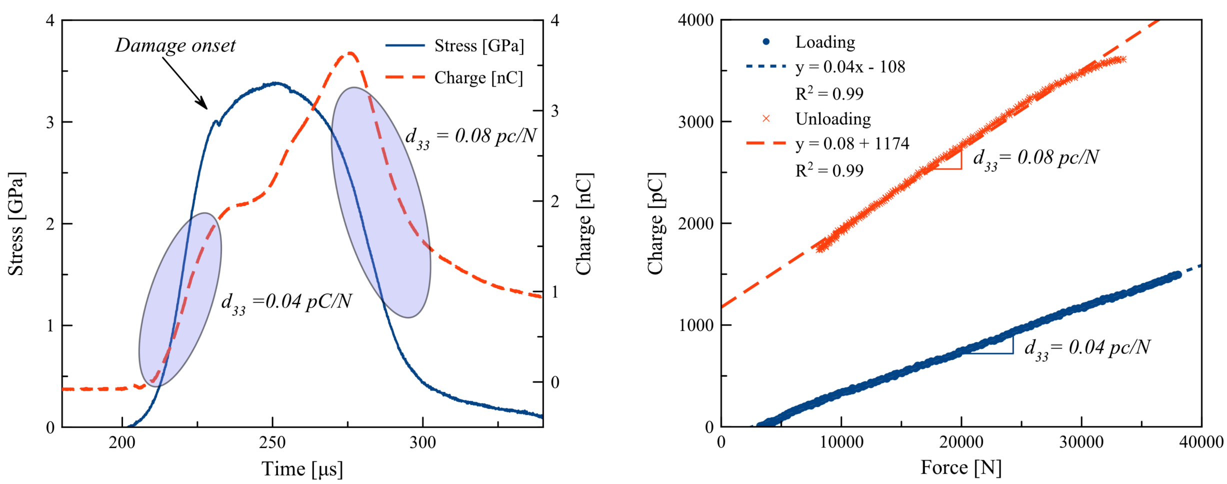


Figure 7. Sample dynamic electromechanical compression test result on SiC (6H) where the sample did not exhibit threshold electrical behavior, but did not reach full comminution on loading.

Table II. Experimental results from the dynamic compressive electromechanical response of single crystal (4H) and (6H) SiC.

| Crystal | ID | Peak Stress [GPa] | Strain Rate [$s^{-1}$] | Peak Charge [nC] | Unload Electric Breakdown | Sample Comminuted |
|---|---|---|---|---|---|---|
| 6H | *vd4* | 3.4 | 5000 | 3.6 | N | N |
| 6H | *vd3* | 2.8 | 4400 | 1.2 | Y | Y |
| 6H | *md6* | 2.8 | 6200 | 2.4 | Y | Y |
| 6H | *md1* | 2.0 | 5000 | 3.7 | Y | Y |
| 4H | *pb9* | 2.8 | 5700 | 1.5 | Y | N |
| 4H | *pb3* | 2.3 | 7600 | 2.8 | Y | N |
| 4H | *pb7* | 2.1 | 7000 | 2.3 | Y | N |
| 4H | *pb10* | 2.0 | 7600 | 2.8 | N | Y |

## SUMMARY

Two hexagonal polytypes of silicon carbide, 4H and 6H were investigated under dynamic compassion using a modified Kolsky bar technique mapping both the mechanical and electrical signal during loading and unloading with damage accumulation. Both polytypes exhibited a threshold behavior that lead to a breakdown of the electric response. The 4H and 6H crystals exhibited similar behavior in the magnitude of stress sustained and resulting damage response, however the experimental conditions that lead to the threshold response differed. The piezoelectric coefficient mapped during loading (and in cases without threshold behavior unloading) was approximately an order of magnitude less than those listed in literature; however this difference as well as variations in the intrinsic piezoelectric response are largely attributed to flaws in the crystalline structure. Damage evolution and the electromechanical response appear to be innately correlated.

## ACKNOWLEDGEMENT

This work was funded by the Army Research Laboratory Award W911NF-06-2-0006 through a sub-award from Hopkins Extreme Materials Institute at the Johns Hopkins University. The author would like to thank Professor K.T. Ramesh and Dr. James McCauley for their discussions and assistance.

## REFERENCES

[1] R. Wyckoff, Crystal Structures, *Interscience,* 1963.
[2] R. Cheung, Silicon Carbide Micro Electromechanical Systems for Harsh Environments, *Imperial College Press,* 2006.
[3] R. Newham, Properties of Materials: Anisotropy, Symmetry, Structure, *Oxford University Press,* 2005.
[4] C. Park, B.-H. Cheong, K.-H. Lee, and K. Chang, Structural and Electronic Properties of Cubic, 2H, 4H, and 6H SiC, *Physical Review B,* **49**, 4485 (1994).
[5] A. Taylor and R. M. Jones, Silicon Carbide - A High Temperature Semiconductor, *Pergamon Press,* 1960.
[6] G. Dhanaraj, K. Byrappa, and V. Prasad, Springer Handbook of Crystal Growth, *Springer,* 2010.
[7] D. Nakamura, I. Gunjishima, S. Yamaguchi, T. Ito, A. Okamoto, H. Kondo, S. Onda, and K. Takatori, Ultrahigh-Quality Silicon Carbide Single Crystals, *Nature,* **430**, 1009-12 (2004).
[8] W. Wesch, Silicon Carbide: Synthesis and Processing, *Nuclear Instruments and Methods in Physics Research Section B: Beam Interactions with Materials and Atoms,* **116**, 305-21 (1996).
[9] K. Karch, F. Bechstedt, P. Pavone, and D. Strauch, Pressure-Dependent Properties of SiC Polytypes, *Physical Review B,* **53**, 13400 (1996).
[10] J. D. Clayton, Modeling Nonlinear Electromechanical Behavior of Shocked Silicon Carbide, *Journal of Applied Physics,* **107**, 013520-20-18 (2010).
[11] P. Zavattieri and H. Espinosa, Grain Level Analysis of Crack Initiation and Propagation in Brittle Materials, *Acta Materialia,* **49**, 4291-311 (2001).
[12] D. Grady and M. Kipp, in High-Pressure Shock Compression of Solids, *Springer*, 1993, 265-322.
[13] G. Ravichandran and G. Subhash, A Micromechanical Model for High Strain Rate Behavior of Ceramics, *International Journal of Solids and Structures,* **32**, 2627-46 (1995).
[14] C. E. Anderson Jr, P. E. O'Donoghue, J. Lankford, and J. D. Walker, Numerical Simulations of SHPB Experiments for the Dynamic Compressive Strength and Failure of Ceramics, *International Journal of Fracture,* **55**, 193-208 (1992).

[15]J. Lankford, W. Predebon, J. Staehler, G. Subhash, B. Pletka, and C. Anderson, The Role of Plasticity as a Limiting Factor in the Compressive Failure of High Strength Ceramics, *Mechanics of Materials,* **29**, 205-18 (1998).
[16]W. Chen and G. Ravichandran, Failure Mode Transition in Ceramics under Dynamic Multiaxial Compression, *International Journal of Fracture,* **101**, 141-59 (2000).
[17]H. Espinosa, A. Patanella, and Y. Xu, Dynamic Compression-Shear Response of Brittle Materials with Specimen Recovery, *Experimental Mechanics,* **40**, 321-30 (2000).
[18]K. Zhang, D. Zhang, R. Feng, and M. Wu, Microdamage in Polycrystalline Ceramics under Dynamic Compression and Tension, *Journal of Applied Physics,* **98**, 023505-05-10 (2005).
[19]N. Bourne, J. Millett, and I. Pickup, Delayed Failure in Shocked Silicon Carbide, *Journal of Applied Physics,* **81**, 6019-23 (1997).
[20]C. Shih, M. Meyers, V. Nesterenko, and S. Chen, Damage Evolution in Dynamic Deformation of Silicon Carbide, *Acta Materialia,* **48**, 2399-420 (2000).
[21]S. Sarva and S. Nemat-Nasser, Dynamic Compressive Strength of Silicon Carbide under Uniaxial Compression, *Materials Science and Engineering: A,* **317**, 140-44 (2001).
[22]H. Wang and K. Ramesh, Dynamic Strength and Fragmentation of Hot-Pressed Silicon Carbide under Uniaxial Compression, *Acta Materialia,* **52**, 355-67 (2004).
[23]H. Luo, W. W. Chen, and A. Rajendran, Dynamic Compressive Response of Damaged and Interlocked SiC–N Ceramics, *Journal of the American Ceramic Society,* **89**, 266-73 (2006).
[24]M. Normandia, Impact Response and Analysis of Several Silicon Carbides, *International Journal of Applied Ceramic Technology,* **1**, 226-34 (2004).
[25]R. Klopp and D. Shockey, The Strength Behavior of Granulated Silicon Carbide at High Strain Rates and Confining Pressure, *Journal of Applied Physics,* **70**, 7318-26 (1991).
[26]D. Grady, Shock-Wave Strength Properties of Boron Carbide and Silicon Carbide, *Le Journal de Physique IV,* **4**, C8-385-C8-91 (1994).
[27]R. Feng, G. Raiser, and Y. Gupta, Shock Response of Polycrystalline Silicon Carbide Undergoing Inelastic Deformation, *Journal of Applied Physics,* **79**, 1378-87 (1996).
[28]R. Feng, G. Raiser, and Y. Gupta, Material Strength and Inelastic Deformation of Silicon Carbide under Shock Wave Compression, *Journal of Applied Physics,* **83**, 79-86 (1998).
[29]G. Yuan, R. Feng, and Y. Gupta, Compression and Shear Wave Measurements to Characterize the Shocked State in Silicon Carbide, *Journal of Applied Physics,* **89**, 5372-80 (2001).
[30]T. Vogler, W. Reinhart, L. Chhabildas, and D. Dandekar, Hugoniot and Strength Behavior of Silicon Carbide, *Journal of Applied Physics,* **99**, 023512-12-15 (2006).
[31]T. Behner, D. Orphal, V. Hohler, C. Anderson Jr, R. Mason, and D. Templeton, Hypervelocity Penetration of Gold Rods into SiC-N for Impact Velocities from 2.0 to 6.2 km/s, *International Journal of Impact Engineering,* **33**, 68-79 (2006).
[32]K. T. Ramesh, in Springer Handbook of Experimental Solid Mechanics, edited by W. N. Sharpe, *Springer*, 2008, 929-60.
[33]W. Chen and G. Ravichandran, Static and Dynamic Compressive Behavior of Aluminum Nitride under Moderate Confinement, *Journal of the American Ceramic Society,* **79**, 579-84 (1996).
[34]G. Ravichandran and G. Subhash, Critical Appraisal of Limiting Strain Rates for Compression Testing of Ceramics in a Split Hopkinson Pressure Bar, *Journal of the American Ceramic Society,* **77**, 263-67 (1994).
[35]V. Cimalla, J. Pezoldt, and O. Ambacher, Group III Nitride and SiC Based MEMs and NEMs: Materials Properties, Technology and Applications, *Journal of Physics D: Applied Physics,* **40**, 6386 (2007).
[36]Y. Goldberg, M. E. Levinshtein, and S. L. Rumyantsev, Properties of Advanced Semiconductor Materials GaN, AIN, InN, BN, SiC, SiGe, *John Wiley & Sons, Inc.,* 2001.

[37]Y. Chinone, S. Ezaki, F. Fujita, and K. Matsumoto, in Amorphous and Crystalline Silicon Carbide II, *Springer*, 1989, 198-206.
[38]J. Suda, H. Sato, I. Shoji, and T. Kondo, in *Materials Science Forum* (Trans Tech Publ, 2009), p. 315-18.
[39]D. Damjanovic, Ferroelectric, Dielectric and Piezoelectric Properties of Ferroelectric Thin Films and Ceramics, *Reports on Progress in Physics,* **61**, 1267 (1998).
[40]S. Ha, P. Mieszkowski, M. Skowronski, and L. Rowland, Dislocation Conversion in 4H Silicon Carbide Epitaxy, *Journal of Crystal Growth,* **244**, 257-66 (2002).
[41]H. Matsunami, Progress in Epitaxial Growth of SiC, *Physica B: Condensed Matter,* **185**, 65-74 (1993).
[42]H. Jacobson, J. Bergman, C. Hallin, E. Janzén, T. Tuomi, and H. Lendenmann, Properties and Origins of Different Stacking Faults That Cause Degradation in SiC Pin Diodes, *Journal of Applied Physics,* **95**, 1485-88 (2004).
[43]T. Ohno, H. Yamaguchi, S. Kuroda, K. Kojima, T. Suzuki, and K. Arai, Direct Observation of Dislocations Propagated from 4H–SiC Substrate to Epitaxial Layer by X-Ray Topography, *Journal of Crystal Growth,* **260**, 209-16 (2004).
[44]S. Izumi, H. Tsuchida, I. Kamata, and T. Tawara, Structural Analysis and Reduction of in-Grown Stacking Faults in 4H–SiC Epilayers, *Applied Physics Letters,* **86**, 202108-08-3 (2005).
[45]K. Koga, Y. Fujikawa, Y. Ueda, and T. Yamaguchi, in Amorphous and Crystalline Silicon Carbide IV, *Springer*, 1992, 96-100.
[46]H. Chen, B. Raghothamachar, W. Vetter, M. Dudley, Y. Wang, and B. Skromme, in *Materials Research Society Symposium Proceedings* (Cambridge Univ Press, 2006), p. 169.
[47]M. J. Loboda, et al., in *Materials Science Forum* (Trans Tech Publ, 2010), p. 291-94.
[48]A. Qteish, V. Heine, and R. Needs, Structural and Electronic Properties of SiC Polytypes, *Physica B: Condensed Matter,* **185**, 366-78 (1993).